Supporting Information for
"Intense oceanic uptake of oxygen during 2014-15 winter convection in the Labrador Sea"

J. Koelling[1], **D.W.R. Wallace**[2], **U. Send**[1], **J. Karstensen**[3]

[1]Scripps Institution of Oceanography, La Jolla, California, USA

[2]Dept. of Oceanography, Dalhousie University, Halifax, NS, Canada

[3]GEOMAR Helmholtz Centre for Ocean Research Kiel, Kiel, Germany

Contents

1. Text S1 to S2
2. Figures S1 to S6

Text S1.

We use data from an Argo float crossing from the boundary into the interior in 2016 to infer a ratio between the gradients of heat and oxygen content, shown in figure S5, using 7 data points from the eddy formation region, and 8 data points at K1 to estimate $\frac{\Delta \int_z O_2}{\Delta \int_z T c_p \rho} = \frac{\int_z \overline{O_2}(K1) - \int_z \overline{O_2}(IC)}{\int_z \overline{T c_p \rho}(K1) - \int_z \overline{T c_p \rho}(IC)}$. The depth range used for the calculation is $100-1400m$, as the deepest available measurement for each profile is between $1400m$ and $1500m$, with the upper limit of integration chosen to avoid seasonal bias due to biology in the upper ocean. The resulting estimate of $\frac{\Delta \int_z O_2}{\Delta \int_z T c_p \rho}$ is $-2.84 \pm 0.59\, mol\ \ (GJ)^{-1}$ (mean and standard deviation).

The lateral heat flux is calculated as the difference between measured heat content from all available mooring data between the surface and 1700m and cumulative surface heat flux from NARR data. An error of $38\, W\ \ m^{-2}$, or $0.5\, GJ\ \ m^{-2}$ over the whole study period, is used for the air-sea flux [*Renfrew et al.*, 2009]. The change in heat content between November 1^{st} and April 5^{th} is $-2.9\, GJ\ \ m^{-2}$, with a cumulative surface flux of $-3.91 \pm 0.5\, GJ\ \ m^{-2}$ from NARR, yielding a lateral heat flux of $1.01 \pm 0.5\, GJ\ \ m^{-2}$.

Corresponding author: Jannes Koelling, `jkoelling@ucsd.edu`

Text S2.

Assuming that bubble fluxes are negligible and the flux is calculated as purely diffusive, the piston velocity k_{O_2} is given by

$$k_{O_2} = \frac{F_{O_2}}{O_2^{sat} - O_2^{sea}} \quad (1)$$

At a saturation of 99%, $O_2^{sat} - O_2^{sea} \sim 3.3 \mu mol L^{-1}$, and an uncertainty of $\pm 2 \mu mol L^{-1}$ for the oxygen measurements will lead to a range for the estimate of k_{O_2} of $\frac{3.3}{5.3}$ - $\frac{3.3}{1.3} \hat{k_{O_2}}$, = 0.62 - 2.54$\hat{k_{O_2}}$, where $\hat{k_{O_2}}$ is k_{O_2} calculated assuming no calibration error. In contrast, with a typical winter surface saturation for oxygen of 95% in the Labrador Sea, $O_2^{sat} - O_2^{sea} \sim 16.5 \mu mol L^{-1}$, and the range of k_{O_2} is $0.89 - 1.14 \hat{k_{O_2}}$, reducing the uncertainty in k_{O_2} by a factor of 7.7.

Figure S1.

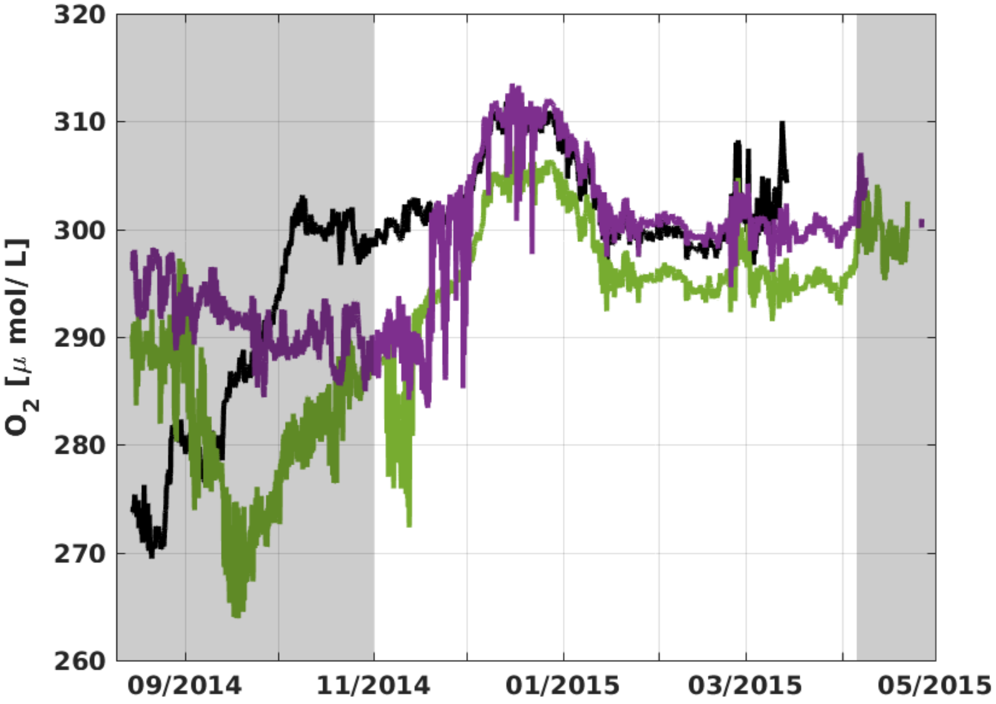

Figure S1. Uncorrected oxygen concentration measured at 10m (black), 60m (green) and 100m (purple). When the mixed layer encompasses all three sensors (after mid-December), short-term variability between sensors agrees well, but there are constant offsets of 4 $\mu mol/L$, 1 $\mu mol/L$, and 5.18 $\mu mol/L$, respectively, between 10m and 60m, 10m and 100m and 60m and 100m, with no significant trend, indicative of instrument drift, in either of those differences. We add a constant value to the 10m and 60m sensors to match the mean value of the 100m sensor. (Note that there is no significance to the choice of 100m as the "true" value, as the O_2 data are further corrected using CTD data, see figure S2).

Figure S2.

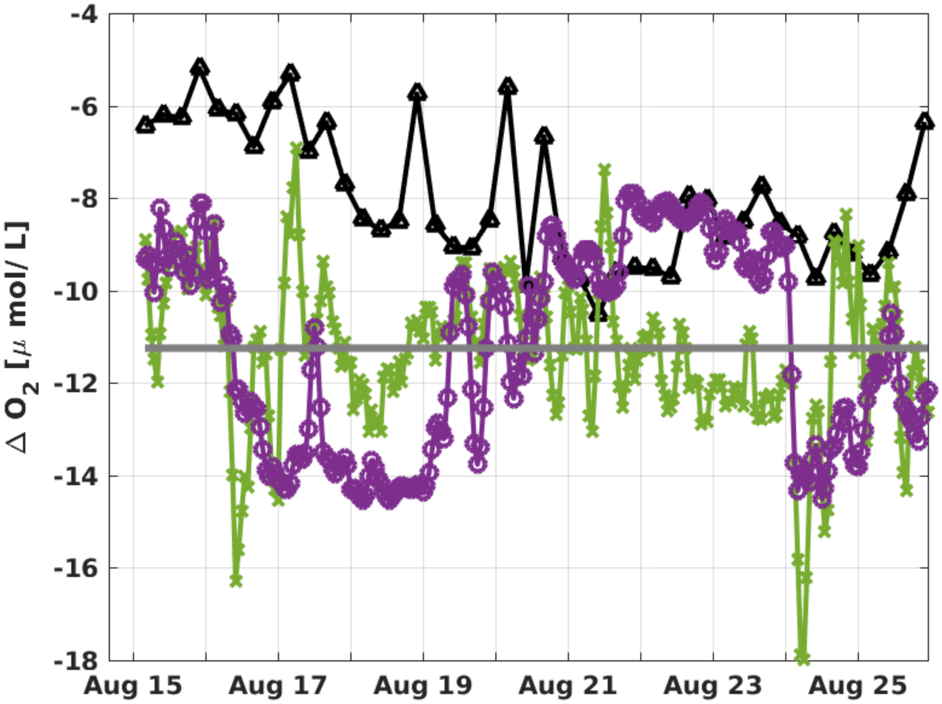

Figure S2. Difference between corrected (see figure S1) mooring data and a CTD profile taken shortly before deployment at 10m (black), 60m (green) and 100m (purple). CTD data were collected during cruise MSM40 onboard RV Thalassa, and were corrected by comparison with water samples analyzed by Winkler titration. The offset $O_2(K1)$ - $O_2(CTD)$ is -8.1, -11.2, -11.3 $\mu mol \ L^{-1}$ at 10, 60 and 100m, respectively. We subtract the mean of the offsets from the two instruments at 60m and 100m, which are well below the mixed layer, from the mooring data to correct for pre-deployment instrument drift. The mean offset is -11.25 $\mu mol \ L^{-1}$, with a standard deviation of 2 $\mu mol \ L^{-1}$, which we use as an estimate of the measurement uncertainty.

Figure S3.

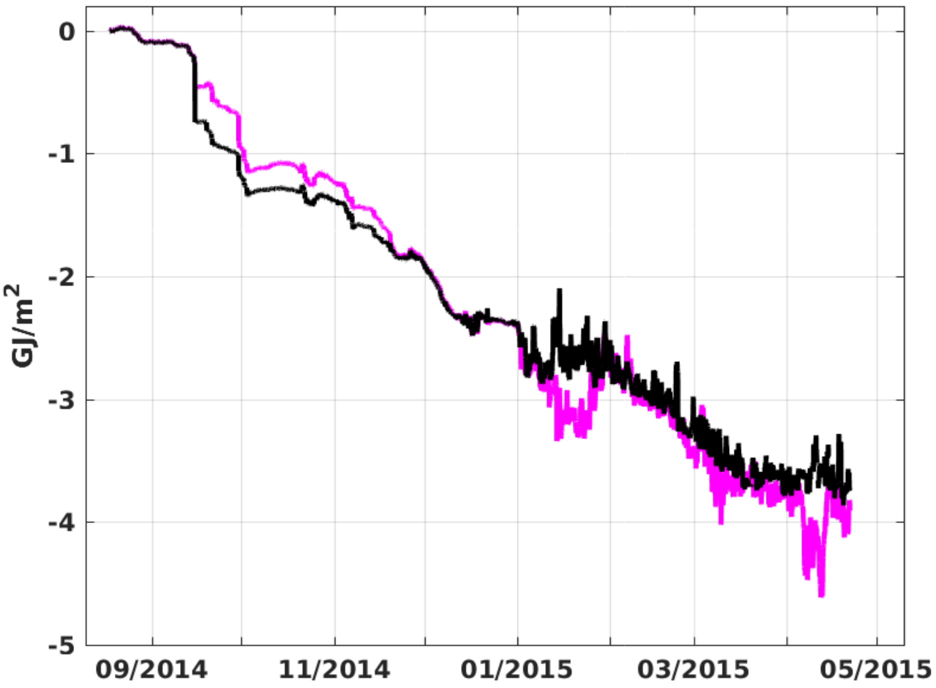

Figure S3. Change in mixed layer heat content calculated from all 11 sensors that are within the mixed layer at each time (black), and calculated from near-surface temperature and z_{MLD} only, analogous to the method used for oxygen (magenta)

Figure S4.

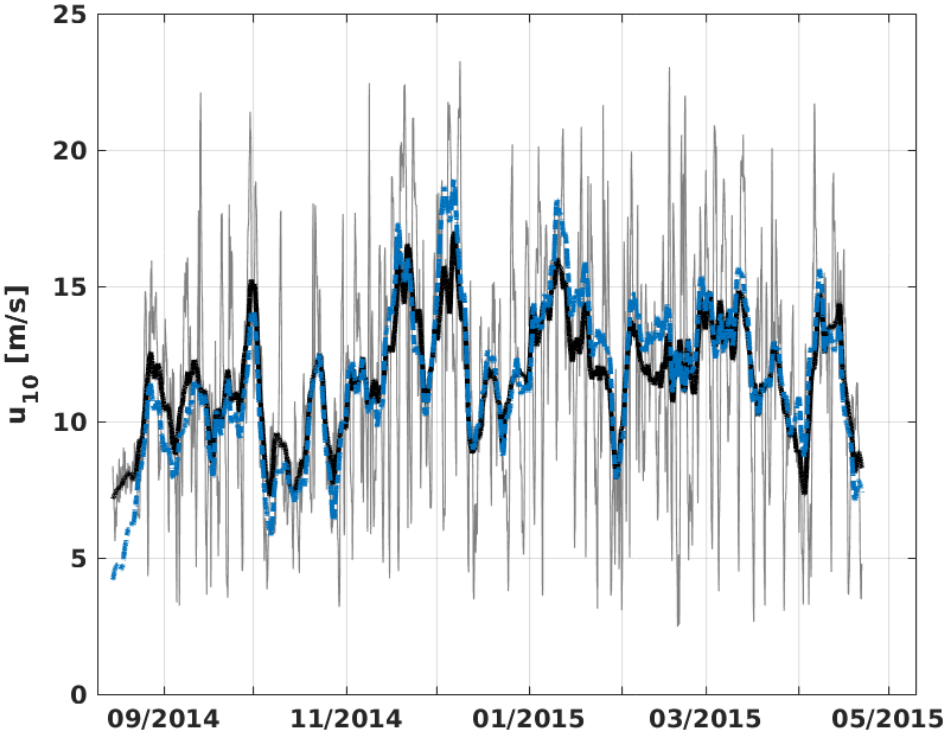

Figure S4. 10m wind speed from NARR, 6-hourly values (grey) and 5-day running mean (black), and 5-day running mean of CCMP winds (blue dash-dotted)

Figure S5.

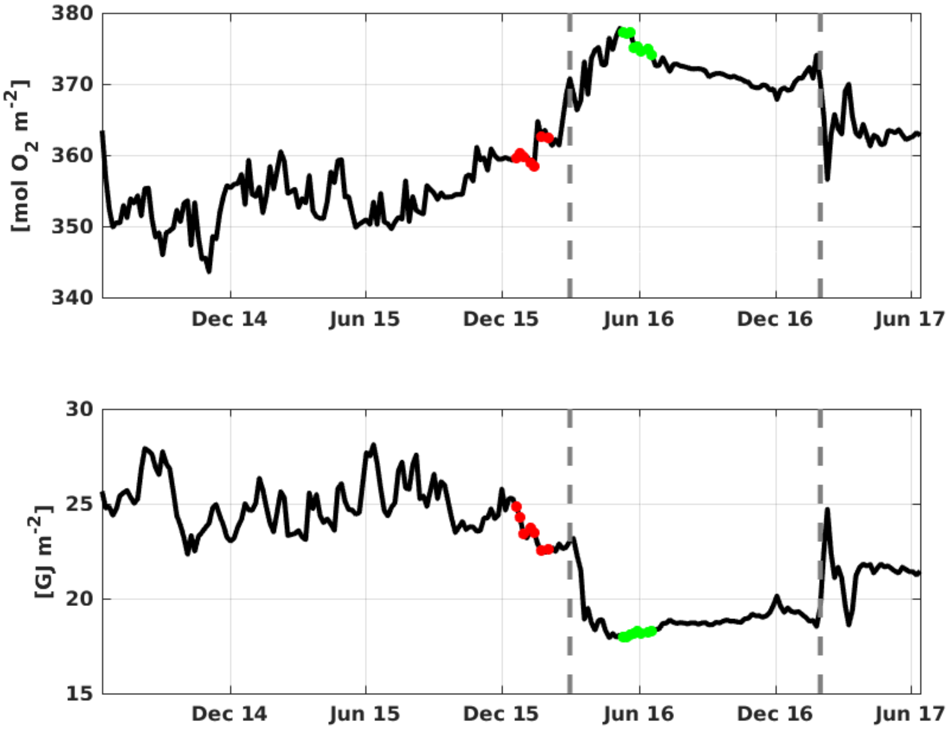

Figure S5. 100-1400m oxygen (top) and heat (bottom) content measured by Argo float #5904989. Gray bars show times when the float entered and subsequently exited the central basin, and symbols show the points used to derive the O_2/heat ratio in F_{adv} for the IC eddy formation region (red) and central Labrador Sea close to K1 (green)

Figure S6.

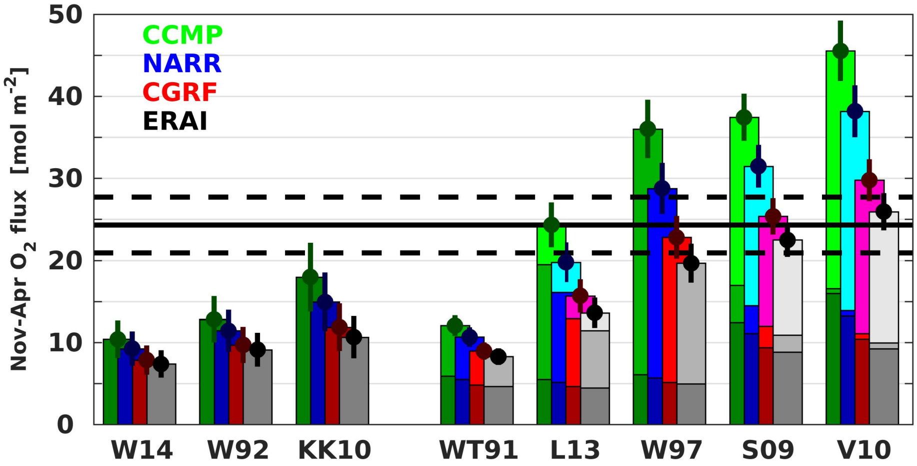

Figure S6. As in figure 3, but assuming no loss of oxygen through lateral transport or respiration, such that $F_{gasex} = \Delta \int O_2$